J Mater Sci (2010) 45:118–123
DOI 10.1007/s10853-009-3900-2

Synthesis and photoluminescence properties of $LiEu(W,Mo)_2O_8:Bi^{3+}$ red-emitting phosphor for white-LEDs

Xiang-Hong He · Ming-Yun Guan · Jian-Hua Sun · Ning Lian · Tong-Ming Shang

Received: 9 March 2009 / Accepted: 15 September 2009 / Published online: 26 September 2009

Abstract $LiEu_{1-x}(W_{2-y}Mo_y)O_8:xBi^{3+}$ series red-emitting phosphors were synthesized by solid state reaction. The structure, morphology, and photoluminescent properties of phosphors were studied by X-ray powder diffraction, scanning electron microscopy, and photoluminescence spectrum, respectively. X-ray powder diffraction analysis showed that the as-obtained phosphors belong to the scheelite structure. The average particle size of the investigated phosphor was about 8 μm. The excitation spectrum exhibits a charge-transfer broad band along with some sharp peaks from the typical 4f–4f transitions of Eu^{3+}. Under excitation of UV, near-UV, or blue light, these phosphors showed strong red emission at 615 nm due to $^5D_0$–$^7F_2$ transition of Eu^{3+}. The incorporation of Mo^{6+} into $LiEuW_2O_8:Bi^{3+}$ could induce red-shift of the charge-transfer broad band and a remarkable increase of photoluminescence. The highest red-emission intensity was observed with $LiEu_{0.80}Mo_2O_8:0.20Bi^{3+}$. Compared with the commercial red-emitting phosphor, $Y_2O_2S:Eu^{3+}$, the emission intensity of $LiEu_{0.80}Mo_2O_8:0.20Bi^{3+}$ phosphor is much stronger than that of $Y_2O_2S:Eu^{3+}$ and its chromaticity coordinates are closer to the standard values than that of the commercial phosphor. The optical properties of $LiEu_{0.80}Mo_2O_8:0.20Bi^{3+}$ phosphor make it attractive for the application in white-light-emitting diodes (LEDs), in particular for near-UV InGaN-based white-LEDs.

X.-H. He (✉) · M.-Y. Guan · J.-H. Sun · N. Lian · T.-M. Shang
School of Chemistry and Chemical Engineering, Jiangsu Teachers University of Technology, 213001 Changzhou, Jiangsu, People's Republic of China
e-mail: hexh@jstu.edu.cn

X.-H. He · M.-Y. Guan · J.-H. Sun · N. Lian · T.-M. Shang
Jiangsu Province Key Laboratory of Precious Metal Chemistry and Technology, Jiangsu Teachers University of Technology, 213001 Changzhou, Jiangsu, People's Republic of China

Introduction

The discovery of the InGaN blue light-emitting diodes (LEDs) chip opened the exciting and challenging research on phosphor-converted-white-LEDs (pc-white-LEDs) as a novel generation of solid-state lighting (SSL) devices [1–3]. The pc-white-LEDs is fabricated by forming a phosphor layer on the output surface of a near-UV or blue-emitting semiconductor chip. In this device, GaN or InGaN chips which emit near-UV light of 370–410 nm or blue light of 450–470 nm are adopted as a primary light source. The eventual performance of pc-white-LEDs' devices strongly depends on the luminescence properties of the phosphors used. The current red-emitting phosphor materials used for pc-white-LEDs include $Y_2O_2S:Eu^{3+}$ [4], Eu^{2+}-activated sulfides (e.g., $CaS:Eu^{2+}$ [5, 6]), $Mg_4O_{3.5}FGeO_2:Mn^{4+}$ [7], and Eu^{2+}- or Ce^{3+}-doped (oxy)nitrides (e.g., $CaAlSiN_3:Eu^{2+}$ [8] and $CaSiN_2:Ce^{3+}$ [9]). Unfortunately, the fluorescent efficiency of $Y_2O_2S:Eu^{3+}$ is about eight times lower than that of $ZnS:Cu^+$, Al^{3+} green and $BaMgAl_{10}O_{17}:Eu^{2+}$ blue-emitting phosphors [4], and its lifetime is inadequate under extended UV irradiation [10]. Eu^{2+}-activated sulfides red-emitting phosphors are chemically unstable and not desirable in efficiency due to releasing of sulfide gas [5, 6]. In addition, sulfide-based phosphors show luminescence saturation with an increasing applied current when incorporated into pc-white-LEDs' devices [11]. $Mg_4O_{3.5}FGeO_2:Mn^{4+}$ phosphor has wide absorption band, but its main emission peak is at about 660 nm which is insensitive to the human eye [7]. As for (oxy)nitride-based red-emitting phosphors, high firing temperatures and high nitrogen

pressures are required for their synthesis [8, 9, 12–14], which result in higher production cost. To overcome the above-mentioned drawbacks, there are extensive efforts worldwide to develop new red-emitting phosphors for pc-white-LEDs' applications, as well as to optimize the existing systems [14–18].

In general, a suitable red-emitting phosphor for pc-white-LEDs should meet the following necessary conditions: the host is stable, the phosphor exhibits strong and broad absorption to output wavelength of LEDs chips (370–470 nm), and the phosphor shows strong red emission [19]. In addition, the full width at half maximum of the emission band should be as small as possible to achieve high luminous output [2]. To obtain a novel red-emitting phosphor with proper Commission Internationale de L'Eclairage (CIE) chromaticity coordinates, it is without doubt that Eu^{3+}-containing compound is the preferable choice because Eu^{3+} usually shows red emission via $^5D_0 \rightarrow {}^7F_2$ transition at about 615 nm.

Double tungstates and molybdates own excellent thermal and hydrolytic stability and are suitable as host for optical materials [20–24]. As a member of this family, europium-based double tungstate, $LiEuW_2O_8$ is a kind of good stoichiometric host-luminescent material with almost no concentration quenching effect [24]. More recently, the development of SSL has lead to a rebirth of interest in this compound for use as phosphor [23, 25, 26], because it gives strong fluorescent under a wide range of excitation wavelengths and of high yield. But high concentration of Eu^{3+} in this compound results in higher production cost, which limits its application in lighting devices. Therefore, it is important to decrease the content of Eu^{3+} in $LiEuW_2O_8$ without reducing its emission efficiency. Moreover, to our best knowledge, less information is available concerning the enhancement of red luminescence in $LiEuW_2O_8$. In this article, first, in an effort to obtain excellent luminescent powders at lower production cost, Bi^{3+} and Mo^{6+} co-doped $LiEuW_2O_8$ was prepared by solid-state method. Then, the effects of Mo^{6+} content on the structure and luminescent properties of $LiEu(W,Mo)_2O_8:Bi^{3+}$ were investigated. The enhanced photoluminescence of $LiEuW_2O_8:Bi^{3+}$ by the substitution of Mo^{6+} for W^{6+} was observed. Finally, the luminescent properties of the composition-optimized material were evaluated by comparison with those of the commercial red-emitting $Y_2O_2S:Eu^{3+}$ phosphor used in white-LEDs.

Experimental

$LiEu_{1-x}(W_{2-y}Mo_y)O_8:xBi^{3+}$ $(x = 0–0.30, y = 0–2.0)$ phosphors were prepared through a typical high temperature solid-state reaction in air. The stoichiometric amount of reactants, Li_2CO_3 (99.9%), WO_3 (99.9%), MoO_3 (99.9%), Eu_2O_3 (99.99%), and $Bi(NO_3)_3{\cdot}5H_2O$ (99.0%) were thoroughly mixed by grinding in an agate mortar and pestle. A small amount of acetone was added during the grindings to obtain homogenous mixtures. The samples were fired at 550 °C for 2 h in a muffle furnace, and then calcined at 800 °C for another 6 h. Finally, the samples are ground into powder for characterizations.

The obtained powder samples were characterized by the powder X-ray diffraction (XRD), scanning electron microscopy (SEM), and photoluminescence spectrum (PL). The XRD was carried out with a Japan Rigaku D-max 2500 diffractometer, using Ni-filtered Cu K_α radiation. A scan rate of 0.02°/s was applied to record the patterns in the 2θ range 10–90°. The particle morphology of the as-synthesized powder was observed by a scanning electron microscope (Hitachi S-3400N Scanning Electron Microscope). The excitation and emission spectra of powders were recorded using fluorescence spectrofluorometer (Varain Cary-Eclipse). All the measurements were performed at room temperature.

Results and discussion

Bi^{3+}-doped $LiEuW_2O_8$ phosphors were successfully synthesized by the solid-state reaction method. The powder XRD patterns of $LiEu_{1-x}W_2O_8:xBi^{3+}$ ($x = 0–0.30$, in steps of 0.025) samples were measured. As examples, the patterns of the phosphors with $x = 0$, 0.05, 0.10, 0.20, and 0.30 are shown in Fig. 1. Curve (a) is very consistent with the JCPDS 48-0886 [$NaY(WO_4)_2$], showing that the sample has a single phase with the scheelite structure. The

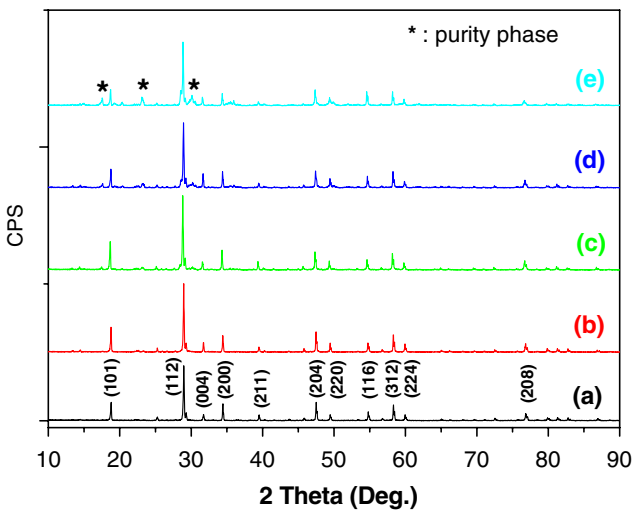

Fig. 1 Powder X-ray diffraction patterns of $LiEu_{1-x}W_2O_8:xBi^{3+}$ with $x = 0$ (*a*), $x = 0.05$ (*b*), $x = 0.10$ (*c*), $x = 0.20$ (*d*), and $x = 0.30$ (*e*)

other four curves are very similar to curve (a), which means that they are isostructure with $LiEu(WO_4)_2$ phase, and Bi^{3+} occupies the same site as Eu^{3+} in the host. The *d* values are slightly different when varying Bi^{3+} content: it may be due to the fact that the Bi^{3+} ion radius (131 pm, eightfold coordination) is a little bigger than that of Eu^{3+} (121 pm, eightfold coordination), which results in a Bi^{3+}–O distance being larger than the Eu^{3+}–O distance, so the *d* values are different. When Bi^{3+} doping concentration is in excess of 10 mol% (i.e., $x > 0.10$), Bi_2WO_6 purity phase appeared and its diffraction intensity increased with increasing of Bi^{3+} doping concentration.

Crystal structure influences the luminescence properties, and hence, we can expect that the progressive replacement of W^{6+} in $LiEuW_2O_8$:$0.02Bi^{3+}$ by Mo^{6+} leads to changes in the photoluminescence property. With this in view, a series of red-emitting phosphors $LiEu_{0.80}(W_{2-y}Mo_y)O_8$:$0.20Bi^{3+}$($y = 0$–2.0, in steps of 0.40) were synthesized and their XRD profiles are shown in Fig. 2. As the *y* value increases, the XRD patterns were found to be similar without showing discernable shifting, because $LiEu_{0.80}(W_{2-y}Mo_y)O_8$:$0.20Bi^{3+}$ system formed whole range solid solutions due to the almost identical ionic radius of Mo^{6+} (41 pm) and W^{6+}(42 pm).

Figure 3 shows the representative SEM micrograph of $LiEu_{1-x}W_2O_8$:xBi^{3+} phosphor. The sample is crystallized quite well, and owns polyhedron morphology and smooth-surface characteristics. All particles are lowly aggregated and its average particle size was about 8 μm.

Figure 4 displays the excitation spectra of $LiEu_{0.80}(W_{2-y}Mo_y)O_8$:$0.20Bi^{3+}$ phosphors ($y = 0$, 0.40, 0.80, 1.20, 1.60, and 2.0) monitored at 615 nm corresponding to $^5D_0 \rightarrow {}^7F_2$ emission of Eu^{3+} ions. The intense broad band can be attributed to the O → (W,Mo) ligand-to-metal charge-

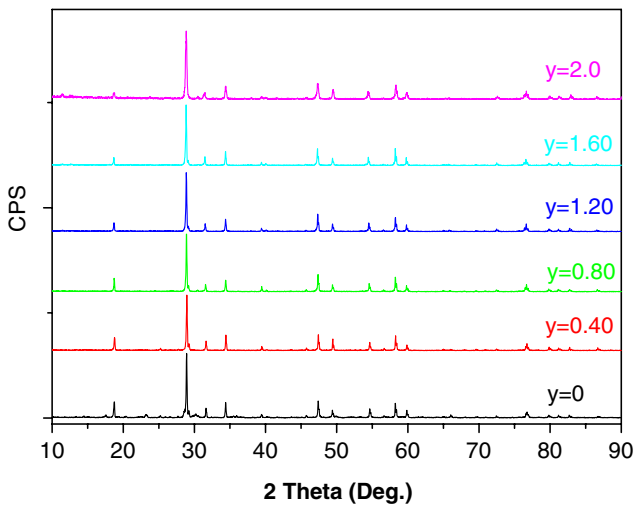

Fig. 2 Powder X-ray diffraction patterns of $LiEu_{0.80}(W_{2-y}Mo_y)O_8$:$0.20Bi^{3+}$ phosphors ($y = 0$, 0.40, 0.80, 1.20, 1.60, and 2.0)

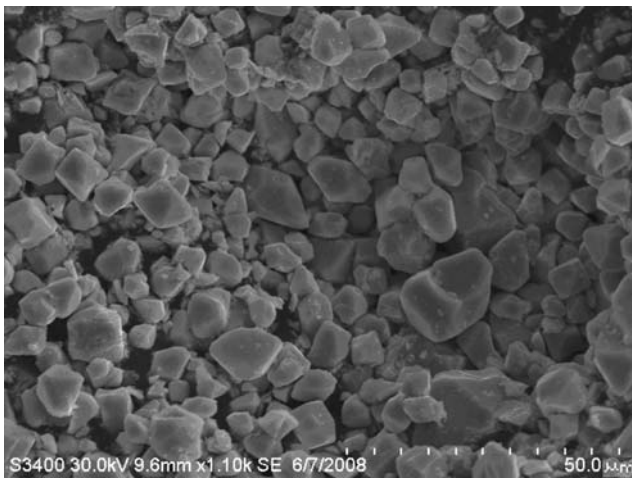

Fig. 3 SEM micrograph of $LiEu_{1-x}W_2O_8$:xBi^{3+} phosphor powder

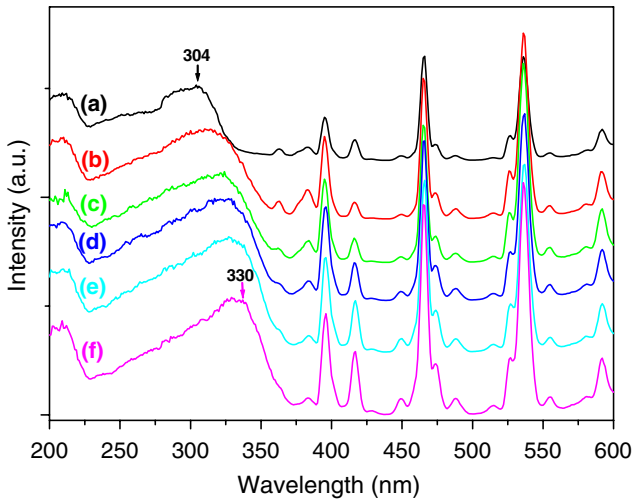

Fig. 4 Effect of Mo^{6+} content on excitation spectra of $LiEu_{0.80}(W_{2-y}Mo_y)O_8$:$0.20Bi^{3+}$ phosphors ($y = 0$, 0.40, 0.80, 1.20, 1.60, and 2.0, for curves (*a*), (*b*), (*c*), (*d*), (*e*), and (*f*), respectively) (monitoring wavelength: $\lambda_{em} = 615$ nm)

transfer transition (LMCT). However, the CT band of Eu^{3+}–O^{2-} was not clearly observed in the excitation spectra, which could be due to possible overlap with that of tungsto-molybdate group. In the range from 360 to 600 nm, all samples show characteristic intraconfigurational 4f–4f transitions of Eu^{3+}: $^7F_0 \rightarrow {}^5L_6$ transition for 395 nm, $^7F_0 \rightarrow {}^5D_3$ for 416 nm, $^7F_0 \rightarrow {}^5D_2$ for 465 nm, and $^7F_1 \rightarrow {}^5D_1$ for 535 nm. With the increase of Mo^{6+} content, the broad band as well as characteristic excitation lines of Eu^{3+} are strengthened. In addition, the broad band systematically shifts toward longer wavelength with increasing Mo^{6+} content (from 304 nm for $LiEu_{0.80}W_2O_8$:$0.20Bi^{3+}$ to 330 nm for $LiEu_{0.80}Mo_2O_8$:$0.20Bi^{3+}$; see Fig. 4). The reason of red-shift of LMCT band may be as follows: with the

replacement of Mo for W, the W–O average distance decreases. In addition, the electronegativity of molybdenum (0.748) is smaller than that of tungsten (0.815). As for M^{n+}–O^{2-} charge transfer, the smaller electronegativity difference between the M^{n+} cation and oxygen, the easier electron transfer from 2p orbital of O^{2-} to the antibonding orbital of M^{n+} cation due to covalency effects [27]. This makes the electrons in the lattice more delocalized and the excitation energy lowers. Thus, the red shift of LMCT band is observed.

As an example, for $LiEu_{0.80}(W_{0.80}Mo_{1.20})O_8$:$0.20Bi^{3+}$ phosphor, excitation at 327 nm into LMCT results in an emission spectrum that does not show any significant differences to the excitation at 395 nm (see Fig. 5). Both the peak position and the shape of the emission spectrum are independent of excitation wavelength. Furthermore, only emission peaks from Eu^{3+} luminescence centers were observed and no emission from Bi^{3+} or tungsto-molybdate group occurred, which indicates there exists only one emission center in this phosphor. These results clearly suggest that an efficient energy transfer from $(W,Mo)O_4$ group to Eu^{3+} has occurred. Figure 6 represents the variations of luminescent intensity of $LiEu_{0.80}(W,Mo)_2O_8$:$0.20Bi^{3+}$ with Mo^{6+} content. The major emission peak of these phosphors was at 615 nm, which corresponds to red emission. Other transitions of Eu^{3+} from the ^5D_J excited levels to ^7F_J ground states, for instance, $^5D_0$–^7F_J is located at 570–720 nm and the $^5D_1$–^7F_J transitions located at 520–570 nm are both very weak, which is advantageous to obtain a phosphor with higher color purity. When the Mo^{6+} content is increased, the red emission at 615 nm of as-prepared phosphors greatly improved. As indicated in Figs. 4 and 6, the incorporation of Mo^{6+} into this phosphor increased the excitation and emission intensity, but did not affect the profiles of spectra. This enhancement may be due to the energy transfer from $(W,Mo)O_4$ group to Eu^{3+}. When the ratio of Mo/W is 2:0, the intensity of red emission reaches a maximum. Moreover, under the excitations of three wavelengths, 395, 465, and 535 nm, emission intensity enhances with the same tendency.

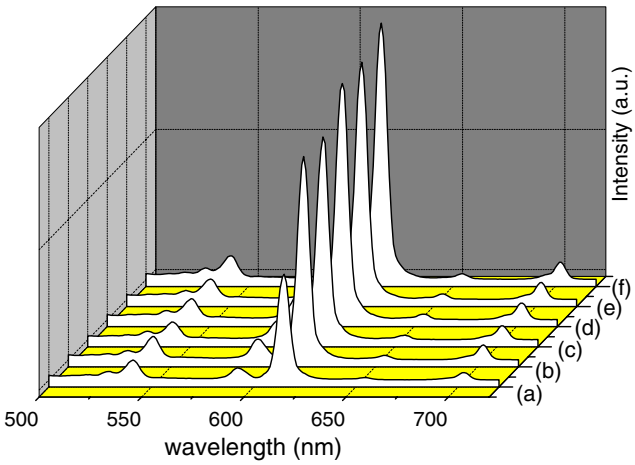

Fig. 6 Effect of Mo^{6+} content on luminescence of $LiEu_{0.80}(W_{2-y}Mo_y)O_8$:$0.20Bi^{3+}$ phosphors ($y = 0$, 0.40, 0.80, 1.20, 1.60, and 2.0, for curves (*a*), (*b*), (*c*), (*d*), (*e*), and (*f*), respectively) ($\lambda_{ex} = 395$ nm)

To evaluate the performance and potential application of this phosphor, we measured and compared the photoluminescence spectra of the composition-optimized $LiEu_{0.80}Mo_2O_8$:$0.20Bi^{3+}$ and the commercial red-emitting phosphor Y_2O_2S:Eu^{3+}(Shanghai Yuelong New Mater. Co. Ltd., China) used in white-LEDs. As shown in Fig. 7, the as-obtained phosphor has higher f–f excitation intensity than that of the commercial red-emitting phosphor. The

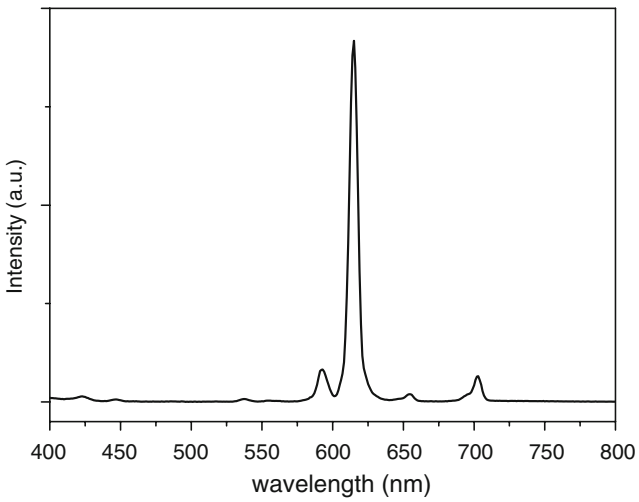

Fig. 5 Emission spectrum of $LiEu_{0.80}(W_{0.80}Mo_{1.20})O_8$:$0.20Bi^{3+}$ phosphor (excitation wavelength: $\lambda_{ex} = 327$ nm)

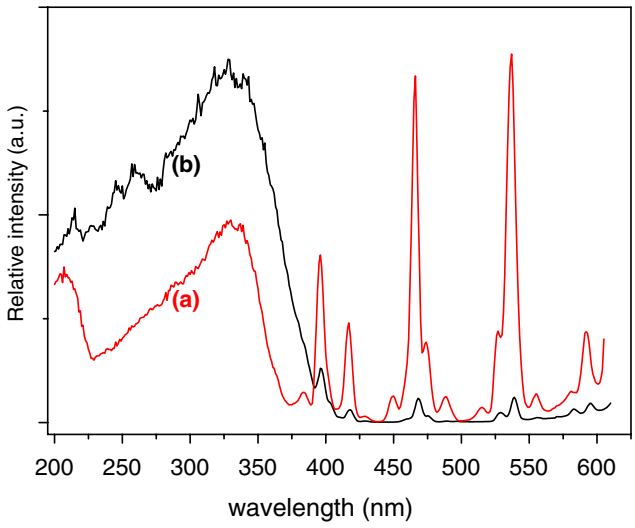

Fig. 7 Excitation spectra of (*a*) $LiEu_{0.80}Mo_2O_8$:$0.20Bi^{3+}$ and (*b*) commercial red-emitting phosphor Y_2O_2S:Eu^{3+}, (*a*) $\lambda_{em} = 615$ nm, (*b*) $\lambda_{em} = 627$ nm

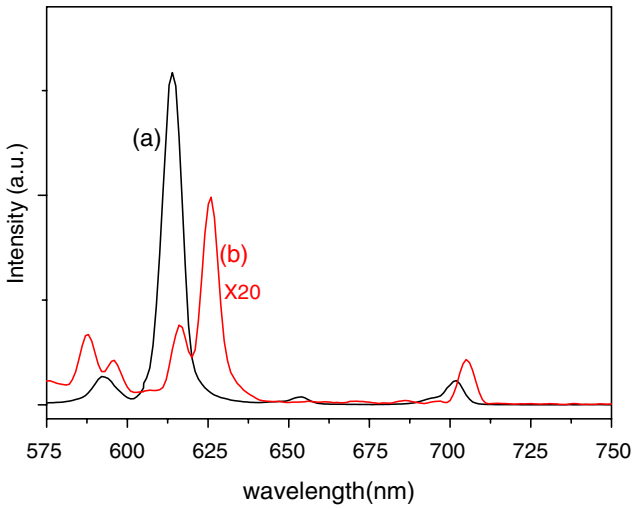

Fig. 8 Emission spectra of (*a*) $LiEu_{0.80}Mo_2O_8:0.20Bi^{3+}$ and (*b*) commercial red-emitting phosphor $Y_2O_2S:Eu^{3+}$ ($\lambda_{ex} = 465$ nm)

main emission peaks at 627 and 616 nm of $Y_2O_2S:Eu^{3+}$ in curve (b) of Fig. 8 are ascribed to Eu^{3+} transition from $^5D_0$ to $^7F_2$ and its strongest peak is at 627 nm. Comparing curve (a) with curve (b) in Fig. 8, the following results can be found. First, the emission intensity of $LiEu_{0.80}Mo_2O_8:0.20Bi^{3+}$ under 465 nm irradiation is about 30 times higher than that of $Y_2O_2S:Eu^{3+}$; while the excitation wavelength turns to 395 nm, the latter's emission intensity is only 12% of the formers. Second, the CIE chromaticity coordinates are calculated to be $x = 0.65$, $y = 0.35$ for $LiEu_{0.80}Mo_2O_8:0.20Bi^{3+}$ and $x = 0.63$, $y = 0.35$ for $Y_2O_2S:Eu^{3+}$. Compared with the National Television Standard Committee (NTSC) standard CIE chromaticity coordinate values for red ($x = 0.67$, $y = 0.33$), it was found that the CIE chromaticity coordinates of $LiEu_{0.80}Mo_2O_8:0.20Bi^{3+}$ was closer to the NTSC standard values than that of $Y_2O_2S:Eu^{3+}$. Consequently, these results indicate that $LiEu_{0.80}Mo_2O_8:0.20Bi^{3+}$ can be used as a better near-UV conversion phosphor as compared to $Y_2O_2S:Eu^{3+}$ in the white-LEDs application.

Conclusions

A class of novel red-emitting $LiEu_{1-x}(W_{2-y}Mo_y)O_8:xBi^{3+}$ phosphors were successfully synthesized by the conventional solid-state reaction technique at high temperature. The average particle size of as-synthesized phosphor was about 8 μm. The excitation spectrum revealed that the absorption is mainly attributed to O → (Mo,W) charge transfer on the range from 220 to 370 nm, and the Eu^{3+} transitions in near-UV and visible regions. Upon excitation with UV or near-UV rays even blue light, these phosphors exhibit strong red luminescence. Both excitation and emission intensity of $LiEuW_2O_8:Bi^{3+}$ were found to increase by incorporation of Mo^{6+}. In addition, the excitation broad band shifts toward longer wavelength with increasing of Mo^{6+} content. The red-emission intensity of $^5D_0$–$^7F_2$ transition of Eu^{3+} reaches a maximum when the relative ratio of Mo/W is 2:0. This improvement can be attributed to energy transfer from $(W,Mo)O_4$ group to Eu^{3+}. The phosphors can be effectively excited by near-UV and blue light and have stronger red emission than the commercial $Y_2O_2S:Eu^{3+}$ used in white-LEDs. The CIE chromaticity coordinates of $LiEu_{0.80}Mo_2O_8:0.20Bi^{3+}$ were closer to the NTSC standard values than that of $Y_2O_2S:Eu^{3+}$. All these suggest composition-optimized $LiEu_{0.80}Mo_2O_8:0.20Bi^{3+}$ phosphor to be suitable candidate for white-LEDs application.

Acknowledgements The authors thank Dr. Jinping Huang of Shanghai Normal University for assistance with the XRD measurements. Financial support from the Natural Science Research Project of the Jiangsu Higher Education Institutions (08KJD150014), the QingLan Project of the Jiangsu Province (2008), and the Basic Research Fund of Jiangsu Teachers University of Technology is gratefully acknowledged.

References

1. Nakamura S, Fasol G (1996) The blue laser: GaN based light emitters and lasers. Springer, Berlin, p 216
2. Jüstel T, Nikel H, Ronda C (1998) Angew Chem Int Ed 37:3084
3. Schubert EF, Kim JK (2005) Science 308:1274
4. Shionoya S, Yen WM (1999) Phosphor handbook. CRC Press, New York
5. Hu Y, Zhuang W, Ye H et al (2005) J Lumin 111:139
6. He XH, Zhu Y (2008) J Mater Sci 43(5):1515. doi:10.1007/s10853-007-2359-2
7. Shi G (2007) Semiconductor light-emitting diodes and solid state lighting. Science Press, Beijing In Chinese
8. Uheda K, Hirosaki N, Yamamoto Y, Naito A, Nakajima T, Yamamoto H (2006) Electrochem Solid State Lett 9(4):H22
9. Toquin RL, Cheetham A (2006) Chem Phys Lett 423:352
10. Neeraj S, Kijima N, Cheetham AK (2004) Chem Phys Lett 387:2
11. Wu H, Zhang X, Guo C, Xu J, Wu M, Su Q (2005) IEEE Photonics Technol Lett 17:1160
12. Xie RJ, Hirosaki N, Kiumra N, Sakuma K, Mitomo M (2007) Appl Phys Lett 90:191101
13. Piao X, Horikawa T, Hanzawa H, Machida K (2006) Appl Phys Lett 88:161908
14. Duan CJ, Delsing ACA, Hintzen HT (2009) Chem Mater 21(6):1010
15. Saradhi MP, Pralong V, Varadaraju UV, Raveau B (2009) Chem Mater 21(9):1793
16. Gundiah G, Shimomura Y, Kijima N, Cheetham AK (2008) Chem Phy Lett 455:279
17. Uhlich D, Plewa J, Jüstel T (2008) J Lumin 128:1649
18. Won Y, Jang HS, Im WB, Jeon DY (2008) J Electrochem Soc 155(9):J226
19. Guo C, Li B, Jin F (1991) Chin J Lumin 12(2):118
20. Macalik L, Hanuza J, Sokolnicki J, Legendziewicz J (1999) Spectrochimica Acta A 55:251

21. Kato A, Oishi S, Shishido T, Yamazaki M, Iida S (2005) J Phys Chem Solids 66:2079
22. Cascales C, Mendez BA, Rico M, Volkov V, Zaldo C (2005) Opt Mater 27:1672
23. Chiu CH, Wang MF, Lee CS, Chen TM (2007) J Solid State Chem 180:619
24. Van Vliet JPM, Blasse G, Brixner LH (1988) J Solid State Chem 76(1):160
25. Wang J, Jing X, Yan C et al (2006) J Lumin 121:57
26. Sivakumar V, Varadaraju UV (2007) J Electrochem Soc 154(1):J28
27. Jorgensen CK (1962) Absorption spectra and chemical bonding in complexes. Pergamon Press, Oxford